Solar Energy Materials & Solar Cells 104 (2012) 121–124

Contents lists available at SciVerse ScienceDirect

Solar Energy Materials & Solar Cells

journal homepage: www.elsevier.com/locate/solmat

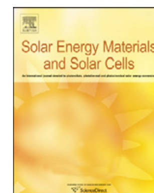

Letter

High resolution saturation current density imaging at grain boundaries by lock-in thermography

S. Rißland*, O. Breitenstein

Max Planck Institute of Microstructure Physics, Weinberg 2, 06120 Halle, Germany

ARTICLE INFO

Article history:
Received 29 February 2012
Received in revised form
3 May 2012
Accepted 9 May 2012

Keywords::
Lock-in thermography
Modeling
IV characteristics
Deconvolution
Local analysis
Grain boundary

ABSTRACT

The electronic properties of multicrystalline solar silicon materials are dominated by low-lifetime defect regions containing recombination-active grain boundaries and dislocations. Besides reducing the carrier collection probability, these regions increase the dark saturation current density J_{01}, which governs the open circuit voltage. By applying lock-in thermography with spatial deconvolution it is shown that the dominant contribution to J_{01} comes from recombination-active grain boundaries and to a lower degree from intra-grain defects like dislocations.

© 2012 Elsevier B.V. All rights reserved.

1. Article

To raise the performance of multicrystalline solar cells it is necessary to understand the recombination effects lowering the efficiency. Crystal defects such as dislocations or grain boundaries (GBs) act as recombination centers and thus lower the local carrier lifetime and increase the local diffusion current described by J_{01}. Due to the macroscopic dimension of grain boundaries, their recombination activity becomes visible in beam-injection methods like electron beam induced current, light beam induced current, and cathodoluminescence imaging. These methods were used to measure the recombination velocity at GBs quantitatively [1–3]. More recently electroluminescence (EL) imaging is also used to image recombination-active defects in solar cells [4]. On the other hand, dark lock-in thermography (DLIT) enables a direct quantitative measurement of the dark current density [5]. Earlier investigations have demonstrated a clear correlation between EL and DLIT in low-lifetime regions, but the J_{01} images obtained from both methods disagreed quantitatively [6]. Since DLIT shows a considerably worse spatial resolution than EL, a direct comparison on microscopic scale was not possible yet.

In this letter, we demonstrate that it is possible to measure the local diffusion current caused by GBs with considerably improved spatial resolution, comparable to that of EL imaging, by dark lock-in thermography (DLIT) in combination with spatial deconvolution. By applying a model proposed by Lax [7] the results are evaluated quantitatively for measuring the recombination velocity at the GBs.

The DLIT measurements are performed using an infrared camera system by Thermosensorik GmbH [8]. The investigated sample is a 3×3 cm^2 sized part of an industrial multicrystalline solar cell (15.6×15.6 cm^2, $J_{sc}=32.9$ A/cm^2, $V_{oc}=618$ mV, $FF=78.3\%$), which contains a high concentration of GBs. The cell is acid textured and possesses screen printed contacts, an aluminum back surface field, and a silicon nitride antireflection layer. The small piece is contacted on the busbar using a four-probe contacting scheme. The used lock-in frequency of 10 Hz leads to a thermal diffusion length of 1.6 mm in the 200 μm thick silicon solar cell. To guarantee a homogeneous emissivity, the surface of the cell was covered with black paint. By measuring DLIT-images at different biases it is possible to separate the different dark current contributions due to their specific current–voltage characteristic by using an algorithm and software code called "Local-IV" [9]. Assuming an ideality factor of two for the depletion region recombination current and neglecting ohmic shunt components, the investigation is based on two DLIT images measured at 550 mV and 600 mV with a spatial resolution of 50 μm per pixel at 25 °C. Though it is well-known that the lifetime in multicrystalline material may depend on the injection level [10], here we assume a constant lifetime in simplest approximation. If the lifetime should be injection-dependent, the DLIT investigations have to be made at an injection level comparable to the

* Corresponding author. Tel.: +49 345 5582692; fax: +49 345 5511223.
E-mail address: rissland@mpi-halle.mpg.de (S. Rißland).

0927-0248/$ - see front matter © 2012 Elsevier B.V. All rights reserved.
http://dx.doi.org/10.1016/j.solmat.2012.05.011

operation condition of the cell. This is roughly the case for our investigations.

The necessary local series resistance (R_s) distribution is evaluated by a combination of EL and DLIT-imaging called RESI [11], which is also implemented in the "Local-IV" code. Based on EL images at 550 mV and 600 mV the local voltage at 600 mV is obtained by applying the code "EL-Fit" after [12], which, together with the DLIT result at 600 mV, enables the calculation of the local R_s distribution according to [11].

To overcome the limitation in spatial resolution due to thermal blurring in DLIT measurements, a 2-dimensional deconvolution algorithm is applied to the measurements [5]. By using a FFT-formalism, a code called "DECONV" [5] converts the in-phase (0°) and the out-of-phase (−90°) DLIT images into a distribution of the locally dissipated power density p. To limit the unavoidable noise in the deconvoluted images, the deconvolution is performed with a Wiener filter having an adjustment parameter K which allows choosing a compromise between spatial resolution and signal-to-noise ratio. Since this procedure generates an artificial overshoot of the power density into the negative close to the grain boundaries, an additional Gaussian blurring of 4 pixels was applied to the results. It has been checked that this deconvolution and subsequent smoothing procedure does not adulterate the quantitative results, neither the intra-grain current density nor the current per unit length of the GBs.

Fig. 1(a)–(c) shows the experimental results measured by DLIT and EL-imaging while biasing with 0.6 V, and Fig. 1(d)–(f) shows calculated images. Deconvolution of (a) and (b) results in the power density distribution (d). The same was done with the 0.55 V DLIT results (not shown here). The recombination-active

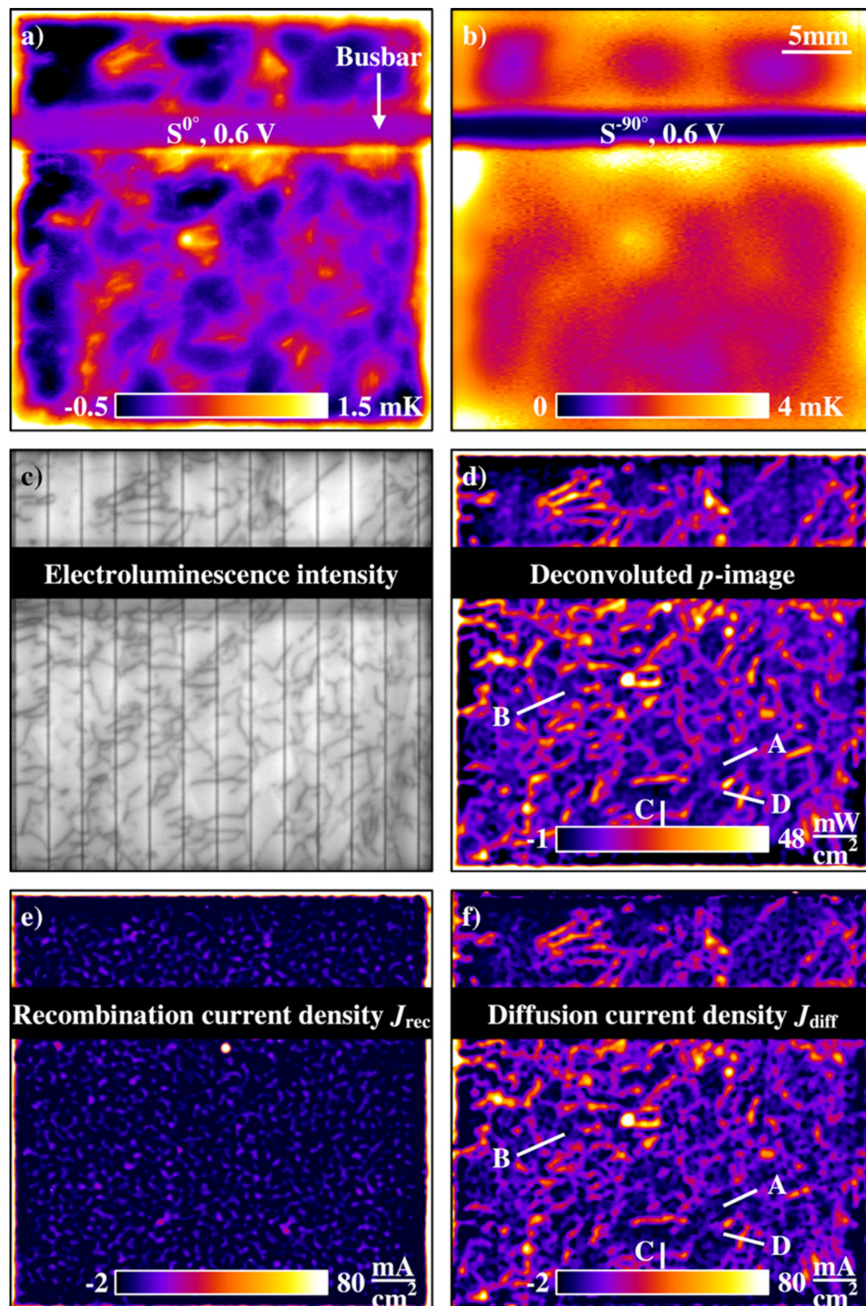

Fig. 1. (a) In-phase and (b) out-of-phase DLIT-image at 600 mV, (c) electroluminescence intensity (arbitrary units), (d) deconvoluted DLIT image (K=1000, Gaussian blurring radius=4 px), (e) recombination current density and (f) diffusion current density at 600 mV (the positions of the evaluated GBs are marked in (d) and (f)).

grain boundaries appear as bright lines in the power density image (d) with a full width at half maximum of 400 μm, whereas in the -90° image previously used for the "Local-IV" procedure the FWHM at 10 Hz is 3.4 mm. Thus, this image (d) has an 8.5 times better spatial resolution than without deconvolution and appears even less blurred than the 0° image (a).

The width of the GB power density signal is still double the thickness of the cell (200 μm). Therefore this region averages over all eventually existing horizontal current components, which may lead to disturbing Peltier contributions in the thermal image [13]. Hence, this power density signal can safely be interpreted as a local measure of current density multiplied with the local bias, which is the presupposition to use it in the "Local-IV" procedure [9]. Applying this procedure to the power density images of 0.55 and 0.6 V and regarding the local series resistance, leads to a diffusion current distribution j_{diff} and a recombination current distribution j_{rec}, which are displayed for 0.6 V in Fig. 1(e) and (f). The recombination current (e) is significantly increased at the cell edges, where the p–n junction crosses the surface, but the inner part of the cell shows only a weak noisy pattern, mainly caused by the noise increase due to the deconvolution procedure. This corresponds to former investigations using the "Local-IV" algorithm [6,9]. The diffusion current (f) obviously dominates the overall current at a bias of 600 mV (see (d)) and is clearly correlated to the recombination-active grain boundaries, which appear dark in the EL-image (Fig. 1(c)). In absence of series resistance problems, it does not matter where the diffusion current flows. Thus the additional j_{diff} at the grain boundaries increases the global diffusion current and thus decreases primarily the open circuit voltage of the solar cell under illumination.

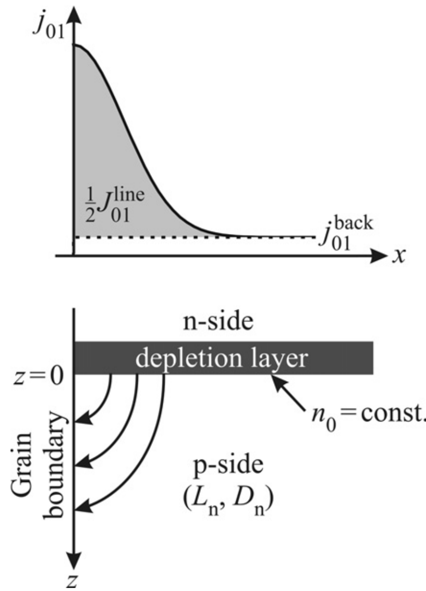

Fig. 2. Electrons injected into the p-side of a p–n junction diffuse towards the grain boundary (GB) with a rate determined by the recombination velocity of the GB and thus increase the local diffusion current density j_{01}.

Simultaneously the light-induced current drops at the GB, which declines the global J_{sc} of the cell. All these local phenomena affect the global cell parameters directly.

For a theoretical interpretation of the influence of recombination at the grain boundaries in multicrystalline solar cells, the two-dimensional GB model developed by Lax was adopted [7], see Fig. 2. The GB is specified by a recombination velocity v_s and is located at $x=0$. As a first assumption the adjacent grains have the same properties and thus the recombination at the GB appears on both sites with half the power. While applying a forward bias the minority carrier density at the p-side close to the depletion layer can be assumed to be constant. The corresponding differential equation with the boundary conditions described above was analytically solved by Lax and results in Eq. (1) for the additional diffusion current line density J_{01}^{line} (in units of A/cm) caused by the GB

$$J_{01}^{line} = \left(\frac{2D_n n_i^2 q}{N_A \pi}\right)\left[\ln\left(\frac{v_s L_n}{D_n}\right) - 1\right] \tag{1}$$

D_n is the diffusion constant for electrons in silicon, n_i is the intrinsic carrier density, q the elementary charge, N_A the doping level and L_n the effective diffusion length in the grains. In infinite distance to the GB the local diffusion current saturation density $j_{01}(x)$ equals the value of the undisturbed p–n junction j_{01}^{back} in Eq. (2)

$$j_{01}^{back} = \frac{qD_n n_i^2}{L_n N_A} \tag{2}$$

Combining the Eqs. (1) and (2) results in the following expression for the recombination velocity v_s:

$$v_s = \frac{j_{01}^{back} N_A}{q n_i^2} \exp\left(\frac{J_{01}^{line} \pi N_A}{2D_n n_i^2 q} + 1\right) \tag{3}$$

j_{01}^{back} and J_{01}^{line} were measured by evaluating linescans perpendicular to the grain boundaries. Since the diffusion current dominates the overall current at a bias of 600 mV in the interesting inner part of the cell, the power density image was interpreted as a pure j_{diff}-distribution. Therefore the noisy pattern caused by the deconvolution does not complicate the determination of the intra-grain diffusion current density.

The linescans were fitted by a Gaussian function with an independent baseline, which represents j_{01}^{back}. By using Eq. (3) under the assumption of $N_A=10^{16}\,\mathrm{cm}^{-3}$, the recombination velocities of the different GBs marked by A through D in Fig. 1(d) were calculated (Table 1). A wide range of more than 3 orders of magnitude can be evaluated for v_s. An analysis of linescans extracted from (d) and (f) results in almost the same values. However, due to the exponential dependency of v_s on J_{01}^{line} the uncertainness raises with increasing v_s. Note that even the recombination velocity might be injection dependent [2] and thus the given results can just be compared with data obtained under the same injection conditions. By averaging the j_{01}^{back} of altogether 25 linescans in this investigated defect-rich region, it could be estimated that only about 40% of the diffusion current stems from the intra-grain regions and 60% from the grain boundaries. Thus the V_{oc} without any grain boundaries (just j_{01}^{back}) of this

Table 1
Evaluation of recombination velocity under the assumption $N_A=10^{16}\,\mathrm{cm}^{-3}$, $D_n=28.25\,\mathrm{cm}^2/\mathrm{s}$ according to Eq. (3).

	j_0^{back} [A cm^{-2}]		J_{01}^{line} [A cm^{-1}]		v_s [cm s^{-1}]	
A	3.26×10^{-13}	$\pm1.22\times10^{-14}$	4.22×10^{-14}	$\pm2.33\times10^{-15}$	1.72×10^{3}	$\pm1.85\times10^{2}$
B	5.53×10^{-13}	$\pm2.43\times10^{-14}$	6.55×10^{-14}	$\pm3.69\times10^{-15}$	5.89×10^{3}	$\pm9.14\times10^{2}$
C	5.48×10^{-13}	$\pm2.80\times10^{-14}$	1.19×10^{-13}	$\pm4.03\times10^{-15}$	2.92×10^{4}	$\pm5.05\times10^{3}$
D	4.74×10^{-13}	$\pm3.59\times10^{-14}$	2.70×10^{-13}	$\pm5.48\times10^{-15}$	2.43×10^{6}	$\pm5.85\times10^{5}$

region would rise by about more than 20 mV, if a homogeneous J_{sc} of 32.9 mA/cm^2 is assumed.

This letter shows the possibility to image the distribution of the different dark current contributions with high spatial resolution and to evaluate them quantitatively. This extends the application field of LIT imaging in dark current characterization of solar cells and offers a deeper insight to recombination activity of GBs and their influence on the overall dark current distribution. The codes of the procedures “Local-IV”, “EL-Fit”, and “DECONV”, which are used in this work, are available from one of the authors (O.B.).

Acknowledgments

This work was financially supported by the German Federal Ministry for the Environment, Nature Conservation and Nuclear Safety and by industry partners within the research cluster “Solar-WinS” (contract no. 0325270C). The content is the responsibility of the authors.

References

[1] C. Donolato, Theory of beam induced current characterization of grain boundaries in polycrystalline solar cells, Journal of Applied Physics 54 (1983) 1314–1322.

[2] G. Micard, G. Hahn, A. Zuschlag, S. Seren, B. Terheiden, Quantitative evaluation of grain boundary activity in multicrystalline semiconductors by light beam induced current: An advanced model, Journal of Applied Physics 108 (2010) 034516.

[3] B.G. Mendis, L. Bowen, Cathodoluminescence measurement of grain boundary recombination velocity in vapour grown p-CdTe, Journal of Physics: Conference Series 326 (2011) 012017.

[4] T. Fuyuki, H. Kondo, Y. Yamazaki, Y. Takahashi, Y. Uraoka, Photographic surveying of minority carrier diffusion length in polycrystalline silicon solar cells by electroluminescence, Applied Physics Letters 86 (2005) 262108.

[5] O. Breitenstein, W. Warta, M. Langenkamp, Lock-in thermography, Springer Series in Advanced Microelectronics 10, Springer-Verlag, Berlin, 2010.

[6] O. Breitenstein, J. Bauer, K. Bothe, D. Hinken, J. Müller, W. Kwapil, M.C. Schubert, W. Warta, Can Luminescence Imaging Replace Lock-in Thermography on Solar Cells? IEEE Journal of Photovoltaics 1 (2011) 159–167.

[7] M. Lax, Junction current and luminescence near dislocation or a surface, Journal of Applied Physics 48 (1978) 2796–2810.

[8] www.thermosensorik.com (2012, May 25).

[9] O. Breitenstein, Nondestructive local analysis of current-voltage characteristics of solar cells by lock-in thermography, Solar Energy Materials and Solar Cells 95 (2011) 2933–2936.

[10] B. Michl, M. Rüdiger, J.A. Giesecke, M. Hermle, W. Warta, M. Schubert, Efficiency limiting bulk recombination in multicrystalline silicon solar cells, Solar Energy Materials and Solar Cells 98 (2012) 441–447.

[11] K. Ramspeck, K. Bothe, D. Hinken, B. Fischer, J. Schmidt, R. Brendel, Recombination current and series resistance imaging of solar cells by combined luminescence and lock-in thermography, Applied Physics Letters 90 (2007) 153502.

[12] O. Breitenstein, A. Khanna, Y. Augarten, J. Bauer, J.-M. Wagner, K. Iwig, Quantitative evaluation of electroluminescence images of solar cells, Physica Status Solidi RRL: Rapid Research Letters 4 (2010) 7–9.

[13] H. Straube, J.-M. Wagner, O. Breitenstein, Measurement of the Peltier coefficient of semiconductors by lock-in thermography, Applied Physics Letters 95 (2009) 052107.